EPJ manuscript No.
(will be inserted by the editor)

Radiative and Collisional Energy Loss, and Photon-Tagged Jets at RHIC

G.-Y. Qin, J. Ruppert, C. Gale, S. Jeon, and G. D. Moore

Department of Physics, McGill University, 3600 university, Montreal, QC, H3A 2T8, Canada

Received: date / Revised version: date

Abstract. The suppression of single jets at high transverse momenta in a quark-gluon plasma is studied at RHIC energies, and the additional information provided by a photon tag is included. The energy loss of hard jets traversing through the medium is evaluated in the AMY formalism, by consistently taking into account the contributions from radiative events and from elastic collisions at leading order in the coupling. The strongly-interacting medium in these collisions is modeled with (3+1)-dimensional ideal relativistic hydrodynamics. Putting these ingredients together with a complete set of photon-production processes, we present a calculation of the nuclear modification of single jets and photon-tagged jets at RHIC.

PACS. PACS-key 25.75.Nq – PACS-key 12.38.Mh

arXiv:0809.2030v2 [hep-ph] 23 Jul 2009

1 Introduction

A wealth of experimental data generated at the Relativistic Heavy Ion Collider have shown that high-p_T hadrons in central A+A collisions are significantly suppressed in comparison with those in binary-scaled p+p collisions [1, 2]. Moreover, the disappearance of back-to-back azimuthal correlations has been observed in central A+A collisions, in contrast to the strong back-to-back correlations in p+p and peripheral A+A collisions [3]. Those results have been attributed to the strong interaction between hard partonic jets produced in the early stage of the collisions and the hot and dense nuclear medium created in the collisions, and they are commonly referred to as jet quenching [4].

A lot of effort has gone into quantitatively calculating the quenching of jets taking place inside the soft nuclear matter. Experimentally, jet quenching can be quantitatively described by measurements of various quantities. One of those is the nuclear modification factor R_{AA} of single-hadron spectra in A+A collisions with respect to that in p+p interactions scaled by the number of binary collisions. In Ref. [5] we presented a systematic calculation of R_{AA} for pions in central and non-central Au+Au collisions at $\sqrt{s} = 200$ AGeV by applying the Arnold, Moore and Yaffe (AMY) [6,7,8] formalism, where the bulk properties of the medium created in those collision are described by (3+1)-dimensional relativistic ideal hydrodynamics [9], which has been shown to give a good description of bulk properties at RHIC. Here, we present our calculation of both radiative and collisional energy loss in the same framework and compare the relative contribution to the nuclear suppression at RHIC [10,11].

Additional information on jet quenching may be obtained by performing correlation measurements, i.e., studying the production of high-p_T hadrons associated with trigger high-p_T particles. One of the most promising suggested triggers is a high p_T photon [12,13]. Hard scatterings in the early stage of the collisions are an important source of photons. If we trigger on such photons, the transverse energy of the away-side associated jet will be determined (note, however, that at next-to-leading order, the kinematics will get contributions from additional $2 \to 3$ processes; we postpone this discussion to a later study.). It is noted that high-p_T photons may be produced from other sources in A+A collisions, such as those involving jet–plasma interaction during jet propagation in the medium and fragmentation of surviving jets after their passing through the medium. In this work, we present a comprehensive study of jet–photon correlations by taking into account all relevant sources for high p_T photon production.

2 Jet energy loss

In our approach, jets (quarks and gluons) evolve in the nuclear medium according to a set of Fokker–Planck type rate equations for their momentum distributions $P(E,t) = dN(E,t)/dE$. Here we write down the generic form of the rate equations [14,15],

$$\frac{dP_j(E,t)}{dt} = \sum_{ab} \int d\omega \left[P_a(E+\omega,t) \frac{d\Gamma_{a\to j}(E+\omega,\omega)}{d\omega dt} - P_j(E,t) \frac{d\Gamma_{j\to b}(E,\omega)}{d\omega dt} \right], \quad (1)$$

where $d\Gamma^{j\to a}(E,\omega)/d\omega dt$ is the transition rate for the partonic process $j \to a$, with E the initial jet energy and ω

the energy lost in the process. The $\omega < 0$ part of the integration incorporates the energy-gain channels. The radiative and collisional parts of the transition rates have been extensively discussed in [5,10].

The initial jet momentum profiles may be computed from pQCD in the factorized formalism. To obtain the momentum spectra of the produced high-p_T hadrons in Au+Au collisions at RHIC, the energy loss of partonic jets in the nuclear medium must be taken into account. This is performed by calculating the medium-modified fragmentation function $\tilde{D}_{h/j}(z, \boldsymbol{r}_\perp, \phi)$ for a single jet,

$$\tilde{D}_{h/j}(z, \boldsymbol{r}_\perp, \phi) = \sum_{j'} \int dp_{j'} \frac{z'}{z} D_{h/j'}(z') P(p_{j'}|p_j, \boldsymbol{r}_\perp, \phi), \quad (2)$$

where $D_{h/j}(z)$ is the vacuum fragmentation function, and $z = p_h/p_j$ and $z' = p_h/p_{j'}$ are two momentum fractions with p_h the hadron momentum and $p_j(p_{j'})$ the initial (final) jet momentum. In the above equation, $P(p_{j'}|p_j, \boldsymbol{r}_\perp, \phi)$ is obtained by solving Eq. (1), representing the probability of obtaining a jet j' with momentum $p_{j'}$ from a given jet j with momentum p_j. It depends on the path taken by the parton and the medium profile along that path, which in turn depends on the location of the jet origin $r_\perp$ and its propagation angle ϕ with respect to the reaction plane. Therefore, one must convolve the above expression over all transverse positions and directions to obtain the final hadron spectra. The initial hard parton densities are determined from the overlap geometry between two nuclei in the transverse plane of the collision zone.

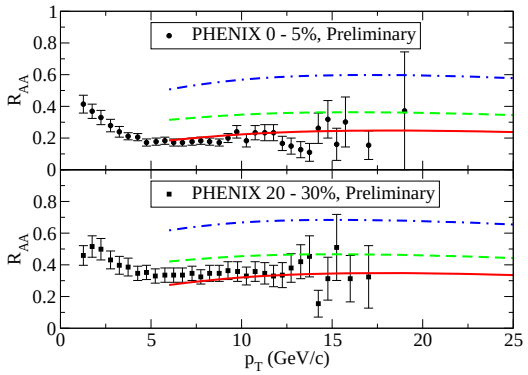

Fig. 1. The nuclear modification factor R_{AA} for neutral pions in central and mid-central collisions (from Ref. [10]). The dashed curves account for only radiative energy loss, the dash-dotted curves for only collisional energy loss and the solid curves incorporate both radiative and collisional energy loss mechanisms.

The calculation of R_{AA} for pions measured at mid-rapidity is shown in Fig. 1 for two different impact parameters, 2.4 fm and 7.5 fm. The experimental data are taken from PHENIX [2] for the most central (0–5%) and mid-central (20–30%) collisions. The strong coupling constant α_s is the only free parameter in our model and it is adjusted in such a way that R_{AA} in most central collisions (Fig. 1, upper panel) is described. The same value, $\alpha_s = 0.27$, is used throughout this work for the calculation of photon production and jet-photon correlations. In this figure, we calculate and compare the relative contribution of induced gluon radiations and elastic collisions to the final pion R_{AA}. One finds that the overall magnitude of R_{AA} is sensitive to both radiative and collisional energy loss while the shape does not show a strong sensitivity.

3 Photon production

In nucleus–nucleus collisions, high-p_T photons may be produced from a variety of sources, namely direct photons, fragmentation photons and jet–plasma photons. Direct photons are produced from hard scatterings in the early stage of the nuclear collisions, and may be computed from pQCD in the factorized formalism. Fragmentation photons are produced from the surviving jets after their passing through the soft medium and may be obtained in a way analogous to the calculation of high-p_T hadrons by replacing the medium-modified hadron fragmentation functions by appropriated photon fragmentation function. Jet–plasma photons are those produced from the processes involving the interaction between jets and the surrounding medium when jets are traversing the plasma. They include induced photon radiation (bremsstrahlung photons) and the conversion from high energy jets by $2 \to 2$ scatterings (conversion photons). Jet–plasma photons may be calculated by incorporating an additional evolution equations for photons in Eq. (1),

$$\frac{dP_\gamma^{\rm jet}(E,t)}{dt} = \int d\omega P_{q\bar{q}}(E+\omega, t) \frac{d\Gamma_{q\to\gamma}^{\rm jet}(E+\omega, \omega)}{d\omega dt}, \quad (3)$$

where $d\Gamma_{q\to\gamma}^{\rm jet}(E,\omega)/d\omega dt$ are the transition rates for jet–plasma channels, including photon bremsstrahlung processes and jet–photon conversion processes, $\Gamma_{q\to\gamma}^{\rm jet} = \Gamma_{q\to\gamma}^{\rm brem} + \Gamma_{q\to\gamma}^{\rm conv}$. The transition rates for induced photon radiation have been discussed in Ref. [6,7,8]. The transition rates for jet–photon conversion processes may be inferred from the photon emission rates in those processes,

$$\frac{d\Gamma_{q\to\gamma}^{\rm conv}(E,\omega)}{d\omega dt} = \sum_f \left(\frac{e_f}{e}\right)^2 \frac{2\pi\alpha_e\alpha_s T^2}{3E} \times \left(\frac{1}{2}\ln\frac{ET}{m_q^2} + C_{2\to2}\right)\delta(\omega). \quad (4)$$

where $m_q^2 = g_s^2 T^2/6$ is the thermal quark mass. In the limit of $E \gg T$, $C_{2\to2} \approx -0.36149$ is a constant [8]. The δ function generates the constraint that the incoming quarks (or anti-quarks) experience no energy loss in the conversion processes.

In Fig. 2, the high-p_T photon production from different channels is shown for most central 0–10% Au+Au collisions ($b = 2.4$ fm) at RHIC, where the number of binary collisions is taken to be $\langle N_{\rm coll}\rangle = 955$ [16]. Our calculations are in good agreement with the data taken from PHENIX [17]. While the direct photons dominate at the very high

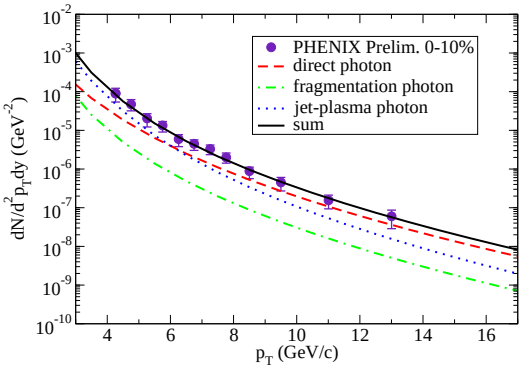

Fig. 2. The contributions from different channels to the photon production in Au+Au collisions at RHIC for $b = 2.4$ fm compared with most 0–10% PHENIX data.

p_T regime ($p_T > 6$ GeV), the presence of the jet–plasma interaction is important for describing the total photon yield in Au+Au collisions at RHIC, especially in the intermediate p_T ($p_T \approx 3$–6 GeV). The thermal photons are expected to be dominant at very low p_T [15,18].

4 Photon-tagged jets

In correlation studies, one of the most interested observables is the per-trigger yield $P(p_T^{\rm asso}|p_T^{\rm trig})$, which represents the conditional probability of producing an associated particle with momentum $p_T^{\rm asso}$ given a trigger particle with momentum $p_T^{\rm trig}$,

$$P(p_T^{\rm asso}|p_T^{\rm trig}) = \frac{P(p_T^{\rm trig}, p_T^{\rm asso})}{P(p_T^{\rm trig})}, \qquad (5)$$

where $P(p_T^{\rm asso})$ and $P(p_T^{\rm trig}, p_T^{\rm asso})$ are the single-particle and two-particle joint probability distributions. As for high-p_T photon–hadron correlations, the associated hadrons are produced from the fragmentation of survival jets after their passing through the nuclear medium, while the triggered photons may come from various sources, as has been discussed in the previous section. Therefore, the photon–hadron correlations depend on jet-photon correlations and the energy loss of the photon-tagged jets.

To take into account all photon sources, we may write the photon yield as the sum of various parts, each associated with a specific source,

$$P(p_T^{\gamma}|p_T^{j}) = \sum_{\rm src} P(p_T^{\gamma}, {\rm src}|p_T^{j}), \qquad (6)$$

where the sources include direct photons, fragmentation photons and jet–plasma photons. As for direct photons, the probability distribution is $P(p_T^{\gamma}, {\rm dir}|p_T^{j}) = \delta(p_T^{\gamma} - p_T^{j})$, since the direct photons have the same momenta as the away-side jets at the production time. The probability function for fragmentation photons is related to the medium-modified photon fragmentation function by $P(p_T^{\gamma}, {\rm frag}|p_T^{j}) = \tilde{D}_{\gamma/j}(z)/p_T^{j}$, where $z = p_T^{j}/p_T^{\gamma}$ is the momentum fraction. As for jet–plasma photons, the probability function $P(p_T^{\gamma}, {\rm jet}|p_T^{j})$ may be obtained by solving Eq. (3) directly.

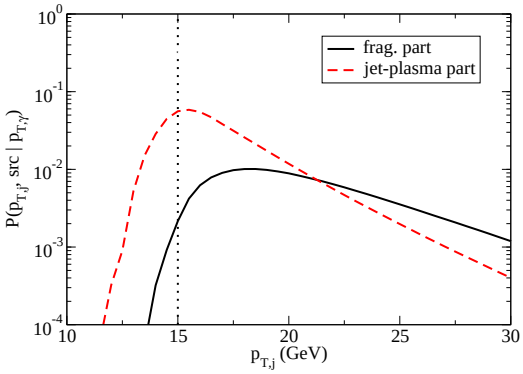

Fig. 3. The contributions from fragmentation photon and jet–plasma photon parts to the initial jet momentum distribution at the production time when we trigger on a photon with momentum $p_T^{\gamma} = 15$ GeV in most central Au+Au collisions at RHIC.

It would be useful to first take a look at the initial jet momentum profiles at production time, given a trigger photon with certain transverse momentum. To compare the relative contributions from different photon sources, we may break the per-trigger yield of the initial jets into different parts,

$$P(p_T^{j}|p_T^{\gamma}) = \sum_{\rm src} P(p_T^{j}, {\rm src}|p_T^{\gamma}). \qquad (7)$$

The above probability function $P(p_T^{j}, {\rm src}|p_T^{\gamma})$ is plotted in Fig. 3 for various photon sources, where the trigger photons have fixed momenta, $p_T^{\gamma} = 15$ GeV. It is obvious that the probability distribution of jets (quarks plus gluons) tagged by direct photons is a δ function with some normalization weight determined by the fraction of direct photons to total photons at 15 GeV. The momentum profiles of jets tagged by fragmentation photons and jet–plasma photons are shown by solid and dashed curves. We find that the initial jets may have higher or lower momenta than the trigger photons. This is attributed to the energy loss or gain experienced by the jets traversing the thermal medium before producing photons by fragmentation and direct jet–plasma interaction. It is found that jets tagged by fragmentation photons dominate at high momentum regime, while jets tagged by jet–plasma photons is prevalent at the relatively lower momentum regime except at 15 GeV.

By applying the medium-modified fragmentation function in Eq. (2) to the above jet momentum profiles, we may obtain the momentum profiles of the associated hadrons. Also, the per-trigger yield of associated hadrons may be written as the sum of different parts associated with dif-

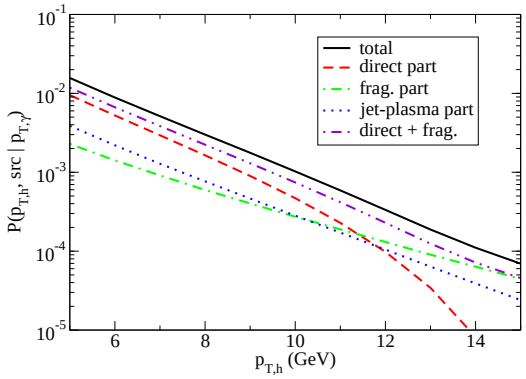

Fig. 4. Various contributions to per-trigger yield of the away-side hadrons when we trigger a photon with momentum $p_T^\gamma = 15$ GeV in most central Au+Au collisions at RHIC.

ferent photon sources,

$$P(p_T^h|p_T^\gamma) = \sum_{\rm src} P(p_T^h, {\rm src}|p_T^\gamma). \quad (8)$$

In Fig. 4, the above probability function $P(p_T^h, {\rm src}|p_T^\gamma)$ for different sources of high-p_T photons are plotted as a function of hadron transverse momenta. We observe that the away-side hadrons at relatively lower p_T regime are mostly produced from those jets that are tagged by direct photons. However, a large amount of away-side hadrons at the higher p_T regime come from those jets tagged by jet–plasma photons and fragmentation photons. Especially, close to the trigger photon momentum, the away side hadron production is dominated by those jets tagged by fragmentation photons. It is noted that the away-side hadrons could have higher momenta than the trigger photon (not shown).

In the above manuscript, we only present some results for photon-tagged jets in Au+Au collisions at RHIC energies. The nuclear modification of the photon-triggered hadron production may be obtained by comparing with similar calculations for p+p collisions. Details of such calculations as well as the comparison to the experimental data will be presented in an upcoming publication [19].

5 Conclusions and discussions

We first calculate the radiative and collisional energy loss of hard partons traversing the quark–gluon plasma and compare the respective size of these contributions to the nuclear suppression in Au+Au collisions at RHIC. The evolution of the thermal medium created in those collisions is modeled by utilizing (3+1)-dimensional relativistic hydrodynamics. It is found that the magnitude of R_{AA} is sensitive to the inclusion of both radiative and collisional energy loss.

Then we apply the same formalism to study the energy loss of photon-tagged jets in Au+Au collisions at RHIC. For high-p_T photon production, we take into account direct photons as well as fragmentation photons and jet–plasma photons. Our results illustrate that the interaction between hard partons and the soft medium are significant for the description of photon data at RHIC. As for the energy loss of photon-tagged jets, we observe the effects due to jet–plasma interaction and fragmentation. Especially, these sources show a significant contribution to the photon-hadron correlations at the high-p_T regime for the associated hadrons. Therefore, it is important to include all photon sources for a full understanding of high-p_T photon–hadron correlations at RHIC. We conclude that both high transverse momentum jets and photons as well as their correlations are very helpful in probing the interaction between hard jets and the surrounding hot and dense medium created in relativistic heavy-ion collisions.

6 Acknowledgements

We thank C. Nonaka and S. A. Bass for providing their hydrodynamical evolution calculation [9]. This work was supported in part by the Natural Sciences and Engineering Research Council of Canada and by the Fonds Nature et Technologies of Quebec.

References

1. PHENIX, K. Adcox *et al.*, Phys. Rev. Lett. **88**, 022301 (2002), arXiv:nucl-ex/0109003.
2. STAR, C. Adler *et al.*, Phys. Rev. Lett. **89**, 202301 (2002), arXiv:nucl-ex/0206011.
3. STAR, C. Adler *et al.*, Phys. Rev. Lett. **90**, 082302 (2003), arXiv:nucl-ex/0210033.
4. M. Gyulassy and X. nian Wang, Nucl. Phys. **B420**, 583 (1994), arXiv:nucl-th/9306003.
5. G.-Y. Qin *et al.*, Phys. Rev. **C76**, 064907 (2007), arXiv:0705.2575.
6. P. Arnold, G. D. Moore, and L. G. Yaffe, JHEP **12**, 009 (2001), arXiv:hep-ph/0111107.
7. P. Arnold, G. D. Moore, and L. G. Yaffe, JHEP **11**, 057 (2001), arXiv:hep-ph/0109064.
8. P. Arnold, G. D. Moore, and L. G. Yaffe, JHEP **06**, 030 (2002), arXiv:hep-ph/0204343.
9. C. Nonaka and S. A. Bass, Phys. Rev. **C75**, 014902 (2007), arXiv:nucl-th/0607018.
10. G.-Y. Qin *et al.*, Phys. Rev. Lett. **100**, 072301 (2008), arXiv:0710.0605.
11. G.-Y. Qin *et al.*, (2008), arXiv:0805.4594.
12. X.-N. Wang, Z. Huang, and I. Sarcevic, Phys. Rev. Lett. **77**, 231 (1996), arXiv:hep-ph/9605213.
13. X.-N. Wang and Z. Huang, Phys. Rev. **C55**, 3047 (1997), arXiv:hep-ph/9701227.
14. S. Jeon and G. D. Moore, Phys. Rev. **C71**, 034901 (2005), arXiv:hep-ph/0309332.
15. S. Turbide, C. Gale, S. Jeon, and G. D. Moore, Phys. Rev. **C72**, 014906 (2005), arXiv:hep-ph/0502248.
16. PHENIX, S. S. Adler *et al.*, Phys. Rev. Lett. **91**, 072301 (2003), arXiv:nucl-ex/0304022.
17. PHENIX, T. Isobe, J. Phys. **G34**, S1015 (2007), arXiv:nucl-ex/0701040.
18. S. Turbide, C. Gale, E. Frodermann, and U. Heinz, Phys. Rev. **C77**, 024909 (2008), arXiv:0712.0732.
19. G.-Y. Qin *et al.*, (in preparation).